AD _____

TECHNICAL REPORT
69-71-CSD

ANALYSIS OF A PARACHUTE WITH A PULLED-DOWN VENT

by

Edward W. Ross, Jr.
Mathematician

February 1969

U. S. ARMY NATICK LABORATORIES
Natick, Massachusetts 01760

FOREWORD

Pulling down the vent of a parachute is a standard method of controlling the drag. This report presents a coherent theory for predicting the shape, drag, and stresses in a steadily descending canopy with a pulled-down vent. A computer program is based on the analysis.

CONTENTS

FIGURES

ABSTRACT

The previous analysis of the author for flat circular canopies in steady descent is here extended to deal with canopies having a pulled-down vent. A general theory is developed, and a partial, approximate solution is found in closed form for certain conditions. The general theory is taken as the basis of a computer program. An example is worked out to demonstrate the use of the program in determining the optimum length of center line. The results are compared with tests and fairly good agreement is obtained. The most interesting outcome is the prediction that the maximum fabric stress is greatly reduced by pulling the vent down.

1. INTRODUCTION

In an earlier paper [1][1], the writer described a procedure for analyzing the shape and stresses in a flat circular parachute during steady vertical descent. This treatment does not assume that the shape is known in advance but finds it and the stresses as functions of the pressure distribution. The resulting computer program gave reasonable results for more or less practical pressure distributions.

The purpose of the present paper is to show how this analysis may be extended to deal with a canopy having a so-called pulled-down vent (see Figure 1). Much of the analysis is identical with that in [1], but there are substantial differences in the edge conditions. These differences make it possible to derive moderately accurate, approximate formulas for the canopy shape in some cases, but increase slightly the difficulty of solving the problem by numerical means.

The analysis of the canopy with the pulled-down vent is described in the next Section. Section 3 contains a derivation of the approximate formulas for the canopy shape. The approximate formulas are not used in the main investigation because they are sometimes inaccurate. Rather, the principal effort in this paper is a numerical analysis leading to a computer solution of the problem, and this is described in Section 4. Section 5 presents the results of the analysis, showing how the drag, shape and stresses depend on the length of the center line that pulls down the vent. The results are discussed in Section 6.

[1]Numbers in brackets designate References at end of paper.

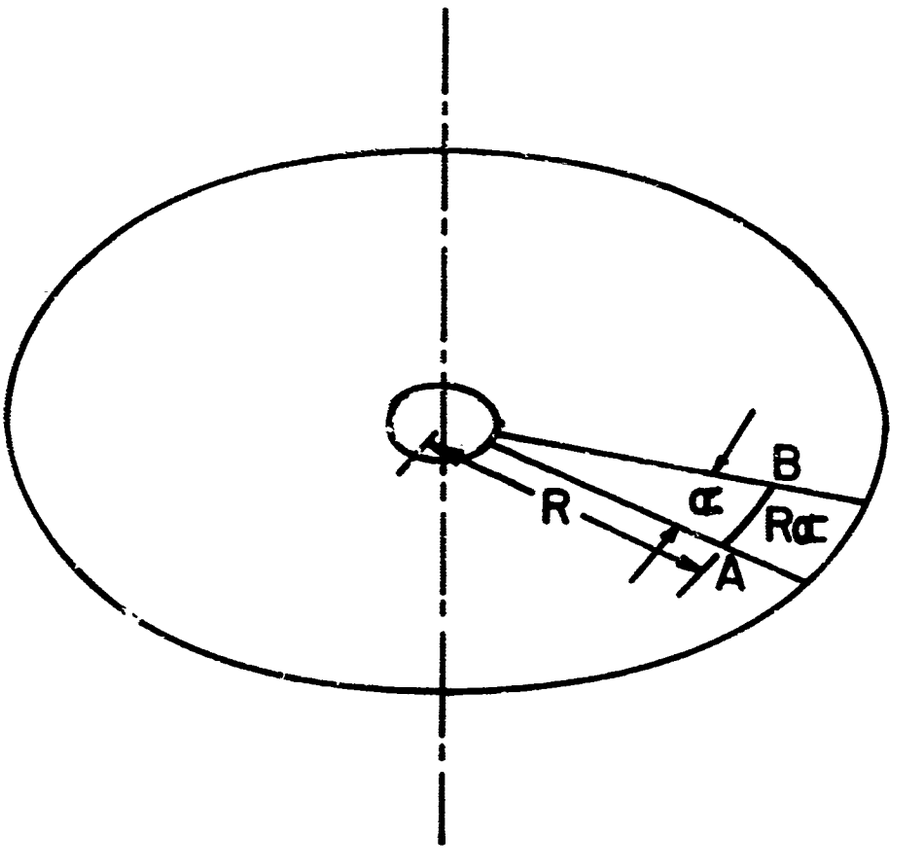

Figure 1. Sketch of Canopy in Flat, Circular (Undeformed) State.

2. ANALYSIS

We shall assume that the canopy may be treated as in [1]. The most important hypotheses introduced in this analysis are listed below:

a. The canopy is descending vertically, and each gore and cord has the same shape and forces as all the others, i.e., the canopy is, roughly speaking, axially symmetric.

b. All meridional forces are borne by the cords, and the gores experience only circumferential stress.

c. All strains are small, although displacements and rotations may be large.

d. The meridional curvature of the deformed gore is negligible compared with the circumferential curvature.

e. Points of a gore that in the flat, circular state lie on a circular arc about the canopy center lie in the deformed state on a plane, circular arc, that plane being perpendicular to the deformed cords.

General sketches of typical undeformed and deformed gores are shown in Figures 1 and 2.

With these assumptions the equations governing the canopy were found in [1], and we reproduce them here without deriving them. The details of the derivation can be found in [1].

$$dr/dR = f \cos \phi \tag{1}$$

$$d\phi/dR = (f/N_s) [pr\alpha - 2N_c \sin(\alpha/2) \sin\phi] \tag{2}$$

$$dN/dR = 2fN_c \cos\phi \sin(\alpha/2) \tag{3}$$

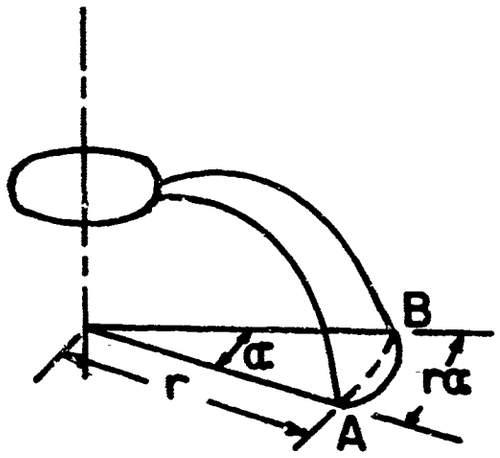

Figure 2. Sketch of a Deformed Gcre.

where

$$f = 1 + t_s, \quad t_s = N_s/E_c \tag{4}$$

and the various quantities are defined in the Nomenclature. The quantity N_c is found as follows:

let

$$A = 1 + [pr\alpha/(2E_f)] - (\pi/2)\,(r/R) \tag{5}$$

If $A < 0$:

$$N_c = E_f \cos\beta\,[(r/R)\,(\beta/\sin\beta) - 1] \tag{6}$$

where β is found by solving

$$\sin\beta - \beta\, r/R + [pr\alpha/(2E_f)] = 0 \tag{7}$$

and

$$\sigma' = 0$$

If $A > 0$:

$$N_c = 0, \quad \beta = \pi/2 \text{ and } \sigma' = R\alpha A/2 \tag{8}$$

Figure 3 shows sketches of the two possible cases that give rise to the alternatives $A < 0$ and $A > 0$. The circumferential fabric stress is expressible in terms of β, as

$$N_f = E_f\,\{\beta(r/R)\csc\beta - 1\} \tag{9}$$

These equations constitute a system of three first-order, non-linear, ordinary differential equations for the quantities r, ϕ and N_s. This differs from common systems of such type in that the right sides of the equations cannot be explicitly written down in terms of R, r, ϕ and N_s, for N_c is expressed implicitly in terms of r and R by Equations (5) to (8).

In order to solve this system, we must append suitable boundary conditions and information about the pressure distribution, p, in the deformed state. So far as our mathematical models are concerned, the only differences

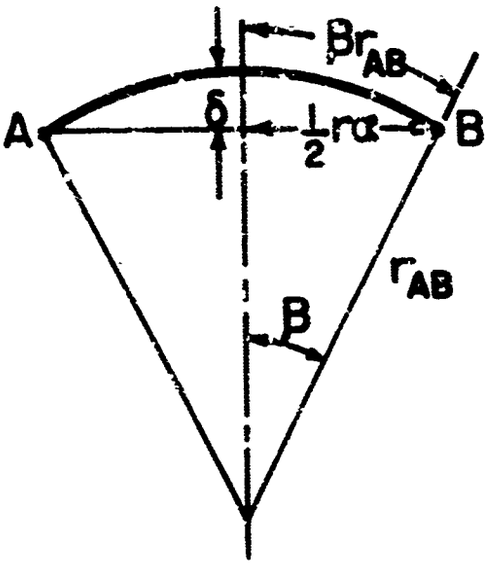

A<0

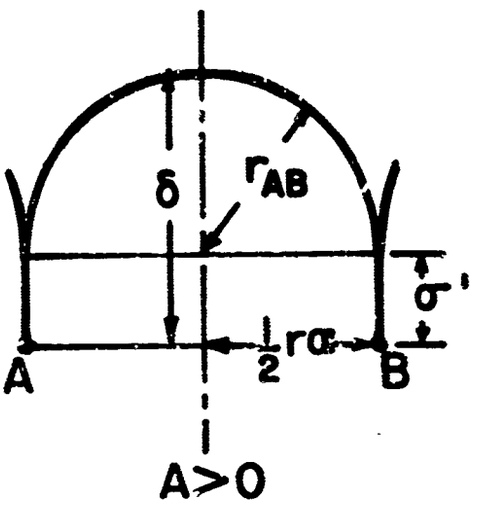

A>0

Figure 3. Possible Cross-Sectional Shapes of a Gore.

between an ordinary flat, circular canopy and one with a pulled-down vent occur in these two phases of the problem. We shall deal first with the boundary conditions, where the most important differences are found.

Figure 4 shows a sketch of the shape of a typical suspension line during steady drop. Four elements make up this shape, the load lines (deformed length L_o), the cords of the canopy itself, the vent lines (deformed length L_i), and the central, pull-down line (deformed length L_p). The geometry of the Figure imposes the following conditions:

$$r(R_i) = L_i \cos[-\phi(R_i)] \tag{10}$$

$$r(R_o) = L_o \sin\theta \tag{11}$$

$$L_p + L_i \sin[-\phi(R_i)] = Z(R_o) + L_o \cos\theta \tag{12}$$

$$Z(R_o) = \int_{R'=R_i}^{R_o} f(R') \sin\phi(R')\, dR' \tag{13}$$

$$\theta = \phi(R_o) - (\pi/2)$$

The tension forces in the various structural elements are shown in Figure 4. N_p is the force in the center line, $N_s(R_i)$ that in each vent line, $N_s(R)$ the variable tension in each cord and $N_s(R_o)$ the force in each load line. Equilibrium requires

$$N_p = GN_s(R_i) \sin[-\phi(R_i)] \tag{14}$$

$$W_L = N_p + GN_s(R_o) \cos\theta. \tag{15}$$

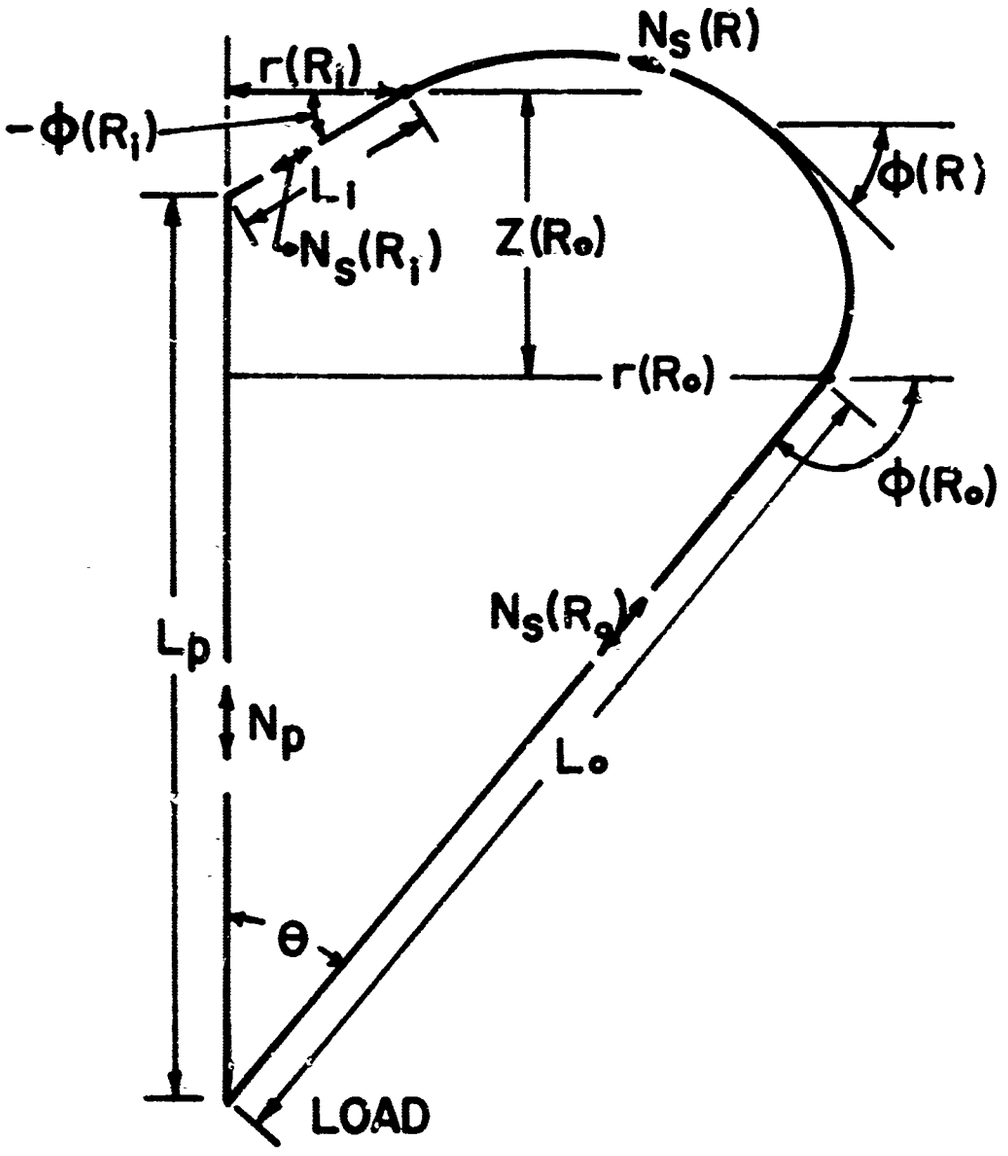

Figure 4. Profile of a Suspension Line, Showing the Forces Acting in the Various Parts.

The linear elastic relations for the structural elements are

$$N_p = E_p \{(L_p/L_p') - 1\} \tag{16}$$

$$N_s(R_i) = E_i \{(L_i/L_i') - 1\} \tag{17}$$

$$N_s(R_o) = E_o \{(L_o/L_o') - 1\}, \tag{18}$$

where E_p, E_i and E_o are the elastic moduli of the center, vent and load lines respectively and L_p', L_i' and L_o' are the undeformed lengths of the corresponding lines.

We may rearrange these equations and eliminate θ with the aid of (13) to get

$$N_p = GN_s(R_i) \sin [-\phi(R_i)] \tag{19}$$

$$L_p = L_p' \{1 + (N_p/E_p)\} \tag{20}$$

$$L_i = L_i' \{1 + [N_s(R_i)/E_i]\} \tag{21}$$

$$r(R_i) = L_i \cos [-\phi(R_i)] \tag{22}$$

together with

$$L_o = L_o' \{1 + [N_s(R_o)/E_o]\} \tag{23}$$

$$r(R_o) + L_o \cos \phi(R_o) = 0 \tag{24}$$

$$L_p + L_i \sin [-\phi(R_i)] = z(R_o) + L_o \sin \phi(R_o) \tag{25}$$

and

$$W_L = N_p + GN_s(R_o) \sin \phi(R_o), \tag{26}$$

We shall now introduce dimensionless quantities as follows:

$$\left.\begin{aligned} R &= xR_i, \quad r = yR_i, \quad R_o = x_oR_i, \quad Z = zR_i \\ L_p' &= \lambda_p'R_i, \quad L_i' = \lambda_i'R_i, \quad L_o' = \lambda_o'R_o \\ L_p &= \lambda_pR_i, \quad L_i = \lambda_iR_i, \quad L_o = \lambda_oR_o \\ N_s &= t_sE_c, \quad N_f = t_fE_f, \quad N_c = t_cE_f, \quad N_p = t_pE_p \\ p &= 2E_fq/R_i, \quad E_f = E_cu_f/E_fR_i \\ E_p &= E_cu_p, \quad E_o = E_cu_o, \quad W_L = wE_c \end{aligned}\right\} \quad (27)$$

Then the differential equation system becomes in dimensionless form

$$dy/dx = f\cos\phi \quad (28)$$

$$d\phi/dx = (f_{uf}/t_s)\,[2q\alpha y - 2t_c \sin(\alpha/2)\sin\phi] \quad (29)$$

$$dt_s/dx = 2f_{uf}\,t_c\cos\phi\sin(\alpha/2) \quad (30)$$

$$f = 1 + t_s \quad (31)$$

and t_c is found as follows: let

$$a = 1 + q\alpha y - [\pi y/(2x)]. \quad (32)$$

If $a < 0$, then $\alpha = 0$ and

$$t_c = [(y/x)(\beta/\sin\beta) - 1]\cos\beta, \quad (33)$$

where β is found by solving

$$\sin\beta - (\beta y/x) + q\alpha y = 0. \quad (34)$$

If $a > 0$, then

$$t_c = 0 \quad (35)$$

$$\sigma = xa\alpha/2. \quad (36)$$

The vent conditions can be written in dimensionless form as

$$t_{p.} = -(G/u_p)\, t_s(1) \sin\phi(1) \tag{37}$$

$$\lambda_p = \lambda_p' (1 + t_p) \tag{38}$$

$$\lambda_i = \lambda_i' [1 + t_s(1)] \tag{39}$$

$$y(1) = \lambda_i \cos\phi(1) \tag{40}$$

and the skirt conditions become

$$\lambda_o = \lambda_o' \{1 + [t_s(x_o)/u_o]\} \tag{41}$$

$$y(x_o) + \lambda_o \cos\phi(x_o) = 0 \tag{42}$$

$$z(x_o) + \lambda_o \sin\phi(x_o) - \lambda_p + \lambda_i \sin\phi(1) = 0 \tag{43}$$

The load relation is then

$$w = t_p u_p + G t_s(x_o) \sin\phi(x_o) \tag{44}$$

We shall take the system (28) to (31) as the equations governing the shape and stresses in the canopy. The numerical procedure, to be described in the next Section, is based on this system. Before undertaking this procedure it is necessary to say a few words about the pressure distribution, $q(x)$, that we shall use. In practice the pressure distribution is not known in advance but has to be found either experimentally or by solving a fluid flow problem jointly with the present elastic deformation problem. In the absence of reliable information about the pressure, we shall proceed as in [1], i.e., we shall assume that q is a polynomial of third degree in ϕ,

$$q = C_o + C_1\phi + C_2\phi^2 + C_3\phi^3$$

and try various choices for the constants C_1, C_2, C_3 and C_o.

3. APPROXIMATE SOLUTION FOR THE SHAPE

A certain amount of numerical experimentation with the system (28)-(31) shows that sometimes t_s is nearly constant and raises the possibility of an approximate solution based on this assumption. We shall investigate this possibility in this Section and see that an approximate solution can be found provided we make some additional hypotheses.

Since the strains are assumed to be small in the cords, we commit little error if we take

$$f \equiv 1.$$

Also the number of gores, G, is usually so large that

$$\sin(\alpha/2) = \alpha/2.$$

With these unessential simplifications we can write the system as

$$dy/dx = \cos\phi \tag{45}$$

$$d\phi/dx = (\alpha u_f/t_s)\,[2qy - t_c \sin\phi] \tag{46}$$

$$dt_s/dx = t_c u_f \cos\phi. \tag{47}$$

We shall assume that the terms containing t_c are small enough to be neglected in (46) and (47). It is not easy to see when this assumption is valid, because more is involved than merely the smallness of t_c itself. Numerical experiments show that the assumption is tolerably accurate provided there is high enough stress in the center line.

In any case with this assumption we obtain that t_s is independent of x and the remaining equations reduce to

$$dy/dx = \cos\phi \tag{48}$$

$$d\phi/dx = Hy \tag{49}$$

$$H = 2q\alpha u_f/t_s \tag{50}$$

This system is rather simple in appearance but still non-linear. If H is constant (i.e., if q is constant), it can be solved by standard methods, giving

$$y = \{1 + (2/H)\,[\sin\phi - \sin\phi(1)]\}^{1/2} \tag{51}$$

$$x = 1 + \int_{\phi'=\phi(1)}^{\phi'=\phi} (Hy)^{-1} d\phi \tag{52}$$

as the solution satisfying the conditions:

$$\text{at } x = 1, \quad y = 1 \quad \text{and} \quad \phi = \phi(1).$$

As yet, H is unknown because t_s is unspecified. To complete the determination of the solution we must evaluate H and $\phi(1)$ by means of the edge conditions. If we neglect the extensions of the various lines, so that

$$\lambda_p = \lambda_p', \quad \lambda_i = \lambda_i' = 1, \quad \lambda_o = \lambda_o',$$

we get from (42) and (43) the conditions

$$\lambda_o' \cos\phi_o + y(\phi_o) = 0 \tag{53}$$

$$\lambda_o' \sin\phi_o - \lambda_p' + \sin\phi(1) + \int_{\phi_i}^{\phi_o} (Hy)^{-1} \sin\phi \, d\phi = 0 \tag{54}$$

$$x_o = 1 + \int_{\phi(1)}^{\phi_o} (Hy)^{-1} \, d\phi. \tag{55}$$

$$\phi_o = \phi(x_o)$$

The solution of these equations for the three quantities H, ϕ_o and $\phi(1)$ requires an iterative process and is at least as complicated as the corresponding steps in the analysis using the original equations.

It is useful to have the formulas (52) to (55) since they serve to check the accuracy of computed results for appropriate conditions. However, they are not generally valid, and the difficulties in meeting the boundary conditions are still present. We conclude that our main effort must still go into a numerical analysis of the original equations, (28) - (31).

4. NUMERICAL ANALYSIS

The fundamental procedure used in this problem is similar to that used for an ordinary, flat circular canopy [1] and is based on a Runge-Kutta solution of the differential equation system (28) to (31). The principal difference is in the treatment of the boundary conditions.

In the earlier case, where there was no center line, there were no vertical forces on the vent, and hence

$$\phi(1) = 0.$$

The condition (43) was not applicable. The procedure was to guess $t_s(1)$, calculate

$$y(1) = 1 + t_s(1),$$

integrate (28) to (31) numerically from $x = 1$ to $x = x_o$ and see whether (42) was satisfied. Various values of $t_s(1)$ were tried, based on the Rule of False Position, until (42) was satisfied with sufficient accuracy.

The present case is more complicated because both $\phi(1)$ and $t_s(1)$ are unknown and have to be chosen so as to satisfy the two conditions (42) and (43). Thus a two-way iterative process is required now. After some experimentation the following iterative scheme was adopted. First, a value was assumed for $\phi(1)$. An iterative process then found the value of $t(1)$ that caused satisfaction of (42). The entire procedure was repeated for different choices of $\phi(1)$ until one was found that also caused (43) to be satisfied. This gave the final solution. Some difficulty was experienced in making good first guesses for $t(1)$ and $\phi(1)$.

Because of the extra iteration the running times for the present calculations were much greater than for the flat, circular case. To keep the running times within reason, it was necessary to use as coarse a mesh as possible in the Runge-Kutta integration. Accordingly, the calculations were all run using a ten-point mesh. The results are surely less accurate than the earlier ones for a flat, circular canopy, but comparison with experimental results and with the approximate solution derived in the next Section indicates that the accuracy is satisfactory for practical purposes.

5. RESULTS

In this Section we describe the computer predictions about the effect on a typical canopy when the vent is pulled down by center lines of different lengths. First, the program developed in [1] for a flat circular canopy was run in order to find the limiting behavior when the center line is either absent altogether or so long that it does not pull the vent down. Then the present program was run for various lengths of center line.

The canopy parameters used in the calculation are those for a G-11-A 100 ft-diameter canopy and are as follows:

R_i = 1.875 ft = vent radius

R_o = 50 ft = skirt radius

G = 120 = number of gores

L_o' = 95 ft = length of load lines

E_c = 2×10^3 lb = modulus of cords

E_f = 3×10^3 lb/ft = modulus of fabric

E_o = modulus of load lines = E_c

ρ = 2.4×10^{-3} lb sec^2/ft^4 = mass density of air

The net pressure was specified in terms of the dimensionless pressure coefficient, C_p, where

$$p = (1/2)\,\rho U^2 C_p \tag{56}$$

and U is the velocity of steady descent. In the present investigation C_p was taken as constant over the whole canopy. In the preliminary runs on flat, circular canopies it was found that $C_p \equiv 1.5$ gave a drag coefficient

$$C_{D_p} = 1.41$$

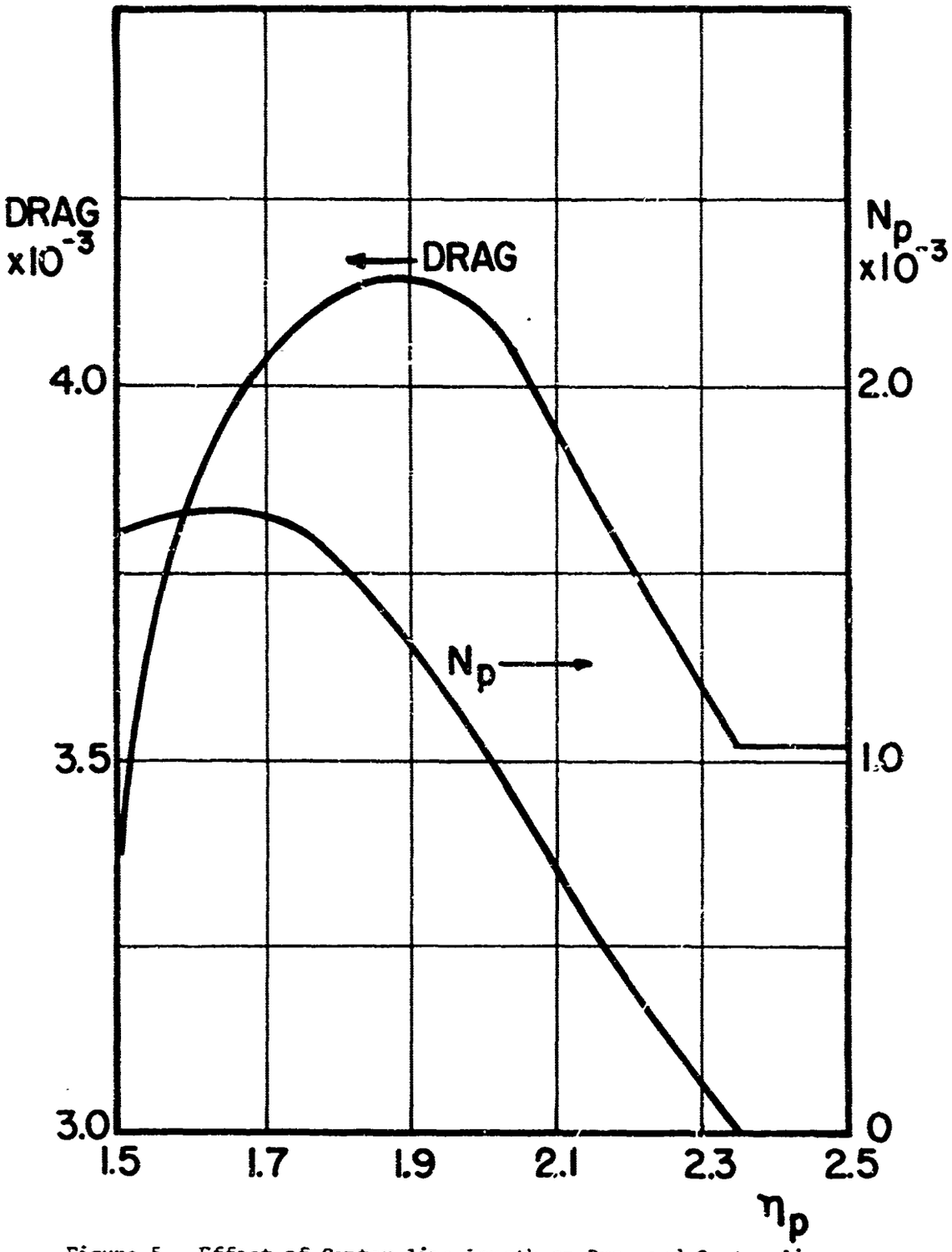

Figure 5. Effect of Center-line Length on Drag and Center-line Tensile Force.

for a considerable range of U-values. This agrees well with experiments on the drag of hemispherical, sheet-metal caps reported by Hoerner [2]. For $C_p \equiv 1.5$ it was found that a drop velocity of

$$U = 24 \text{ ft/sec}$$

caused a drag of about 3500 pounds, which is a commonly accepted value for the load. These values,

$$C_p \equiv 1.5$$

$$U = 24 \text{ ft/sec}$$

were therefore adopted as more or less standard conditions for this canopy and were used in the program for the pull-down vent as well.

The main subject of study in this analysis of the pull-down vent was the effect of the center line length. The elasticity of the center line was taken as

$$E_p = 1.7 \times 10^4 \text{ lb}$$

and the length of the center line was varied in the range $1.5 \leq L_p'/R_o \leq 2.35$. Most of the runs were made with the standard values of C_p and U, but some runs were made at other values to assess the effects of velocity or pressure changes. The results are shown in Figures 5 - 9. In these Figures the center line length is expressed in terms of η_p, where

$$\eta_p = L_p'/R_o.$$

Figure 5 shows how the canopy drag and center line tension are affected by changes in the center line length. A maximum drag of about 4150 lb, corresponding to $C_{D_o} = .739$, is found when $\eta_p = 1.88$ or $L_p' = 94$ ft. This represents an 18% increase over the flat, circular values.

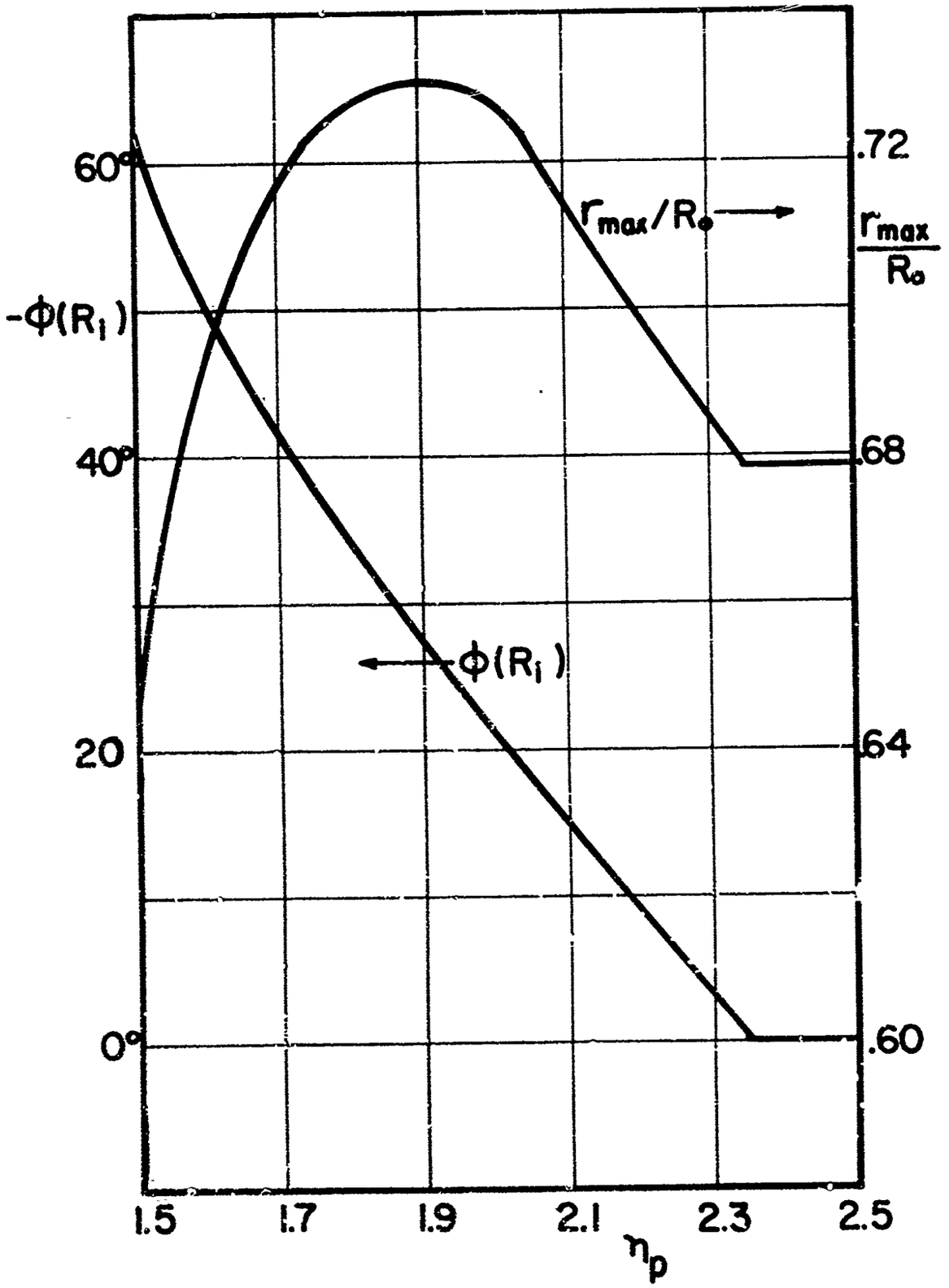

Figure 6. Effect of Center-line Length on Maximum Radius and Cord Angle at the Vent.

$$\text{Drag} = 3530 \text{ lb}$$

$$C_{D_o} = .651$$

The center line tension force, N_p, reaches a maximum of about 1670 lb, when $\eta_p = 1.65$, and drops to zero at the flat, circular value, $\eta_p = 2.35$. The configuration of maximum drag, $\eta_p = 1.88$, gives a control line force, $N_p = 1360$ lb.

The influence of η_p on two geometrical parameters is shown in Figure 6. The ratio of the maximum radius to the flat, circular radius, r_{max}/R_o, reaches its greatest value (.731) at $\eta_p = 1.9$. The corresponding value for a flat, circular canopy is seen to be

$$R_{max}/R_o = .679.$$

The angle of the lines at the vent, $\phi(x_i)$, is seen to change almost linearly from $\phi(x_i) = -61^\circ$ to $\phi(x_i) = 0^\circ$ as η_p increases from 1.5 to 2.35. Incidentally, the angle of the lines at the skirt, $\phi(x_o)$, is almost independent of η_p and has the value

$$\phi(x_o) = 110^\circ$$

The profiles of the canopy lines are shown in Figure 7. We see that the maximum drag corresponds to a shape ($\eta_p = 1.88$) where the vent is pulled down about halfway to the skirt. The constancy of $\phi(x_o)$ is easily observable in this Figure.

The effect of η_p on the cord strain distribution is shown in Figure 8. As the center line is made shorter (i.e., η_p decreases) the tension in the cords becomes more nearly constant. When $\eta \leq 2$, we have the conditions under which the approximations of Section 3 are valid. The cord strain remains

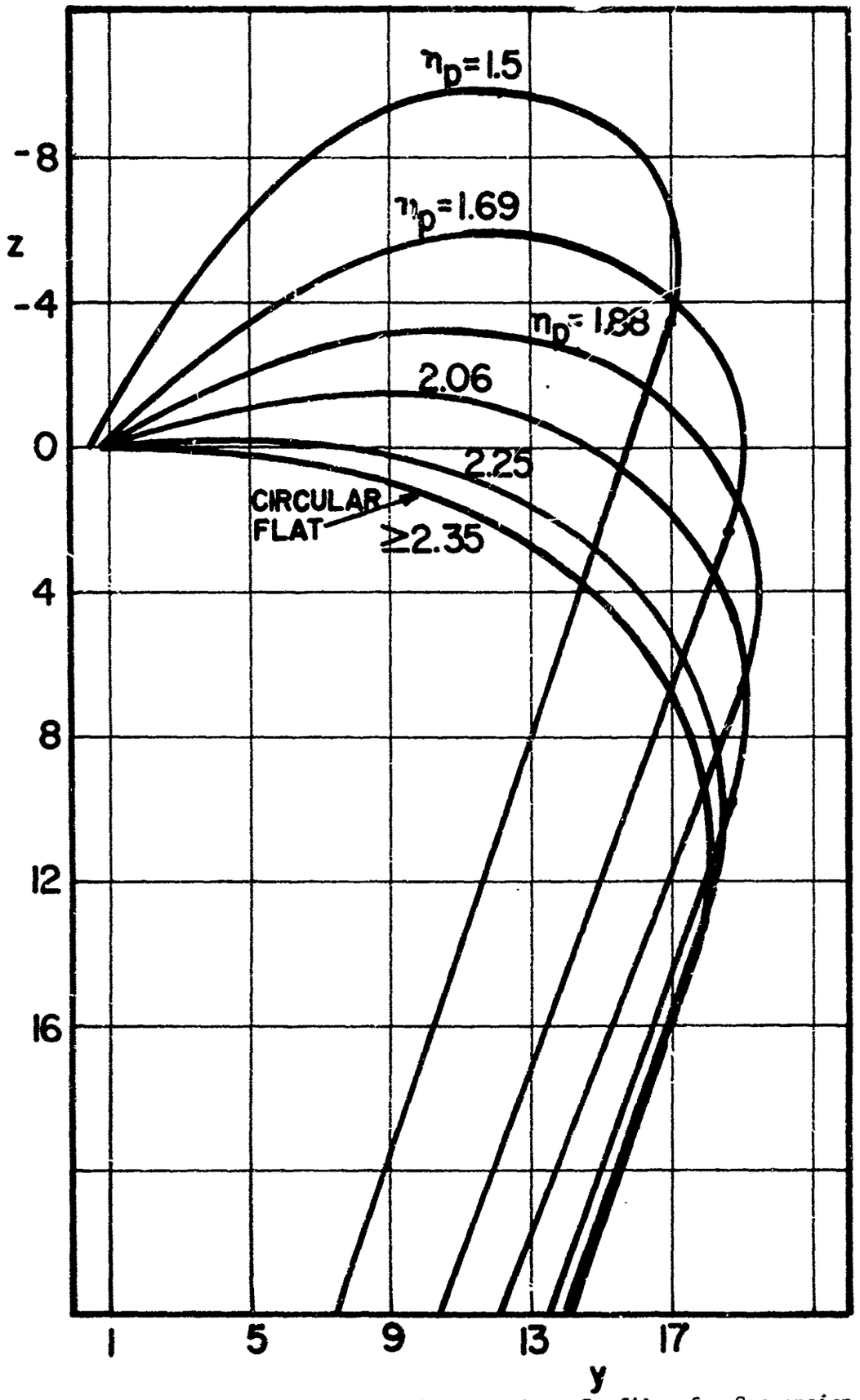

Figure 7. Effect of Center-line Length on Profile of a Suspension Line.

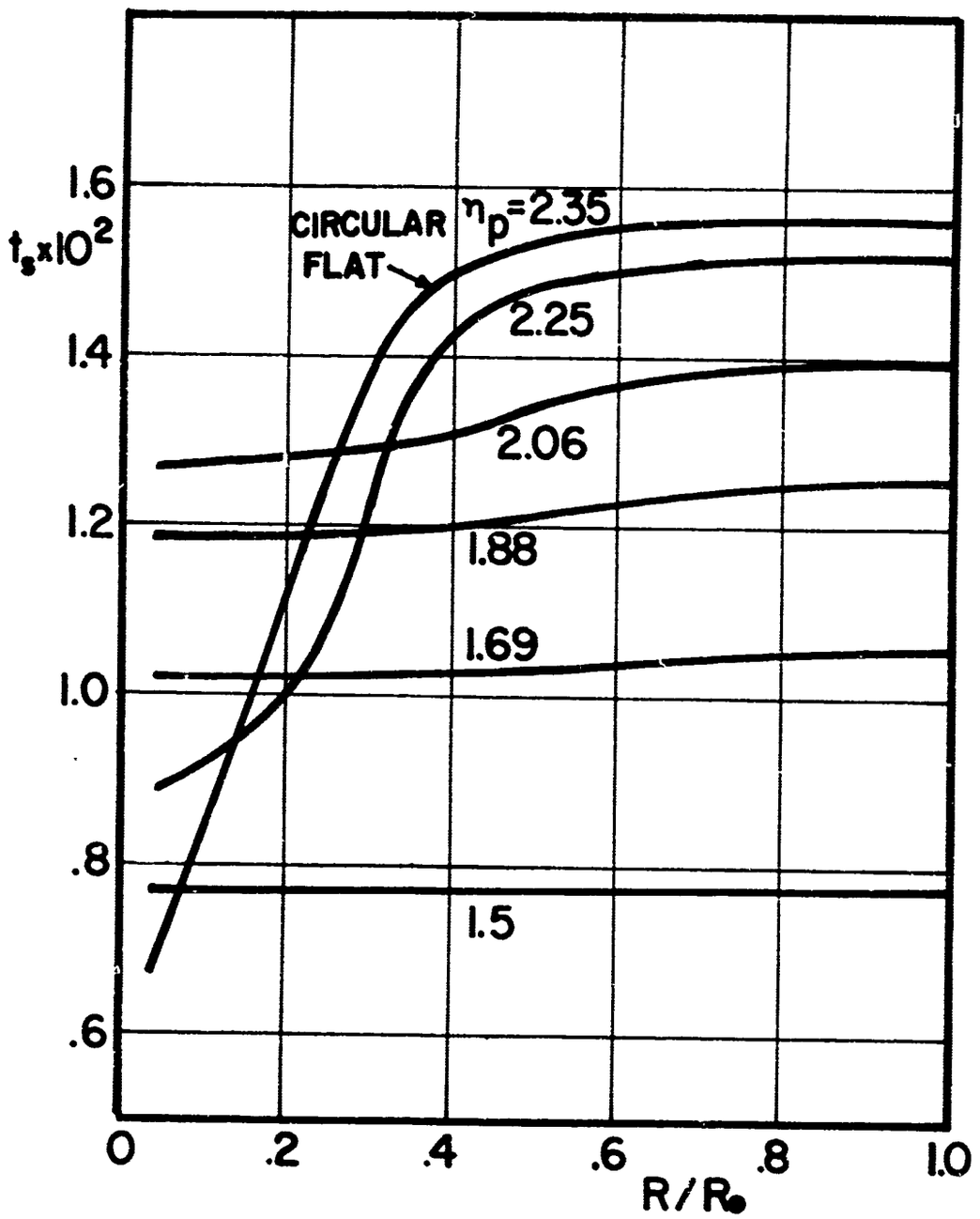

Figure 8. Effect of Center-Line Length on the Distribution of Cord Tensile Force.

fairly constant near the skirt in all cases, but as η_p approaches the flat, circular value the cord strain drops rapidly near the vent.

The most spectacular effect of pulling down the vent is seen in Figure 9, which shows (on a semi-logarithmic plot) the fabric strain distribution. We observe that, as the vent is pulled down, the location of maximum fabric strain is shifted outward (toward the skirt) and the fabric strain itself is greatly reduced. For instance, if η_p is decreased from 2.35 to 1.88 the maximum value of t_f is reduced to about 7% of its previous value. Further shortening of the center line, from $\eta_p = 1.88$ to $\eta_p = 1.5$, causes the maximum t_f to move outward almost to the skirt and continue decreasing, although the rate of decrease is slower than before.

The effects of changing the drop velocity, U, or the assumed constant pressure, C_p, are essentially the same since both enter the calculation only via the formula for the pressure (56). Moderate changes in either quantity cause negligible changes in shape, and the changes in stress and drag are just proportional to those in the pressure. This conclusion is not valid if very large changes occur in C_p or U, or if C_p is permitted to vary substantially with position on the canopy.

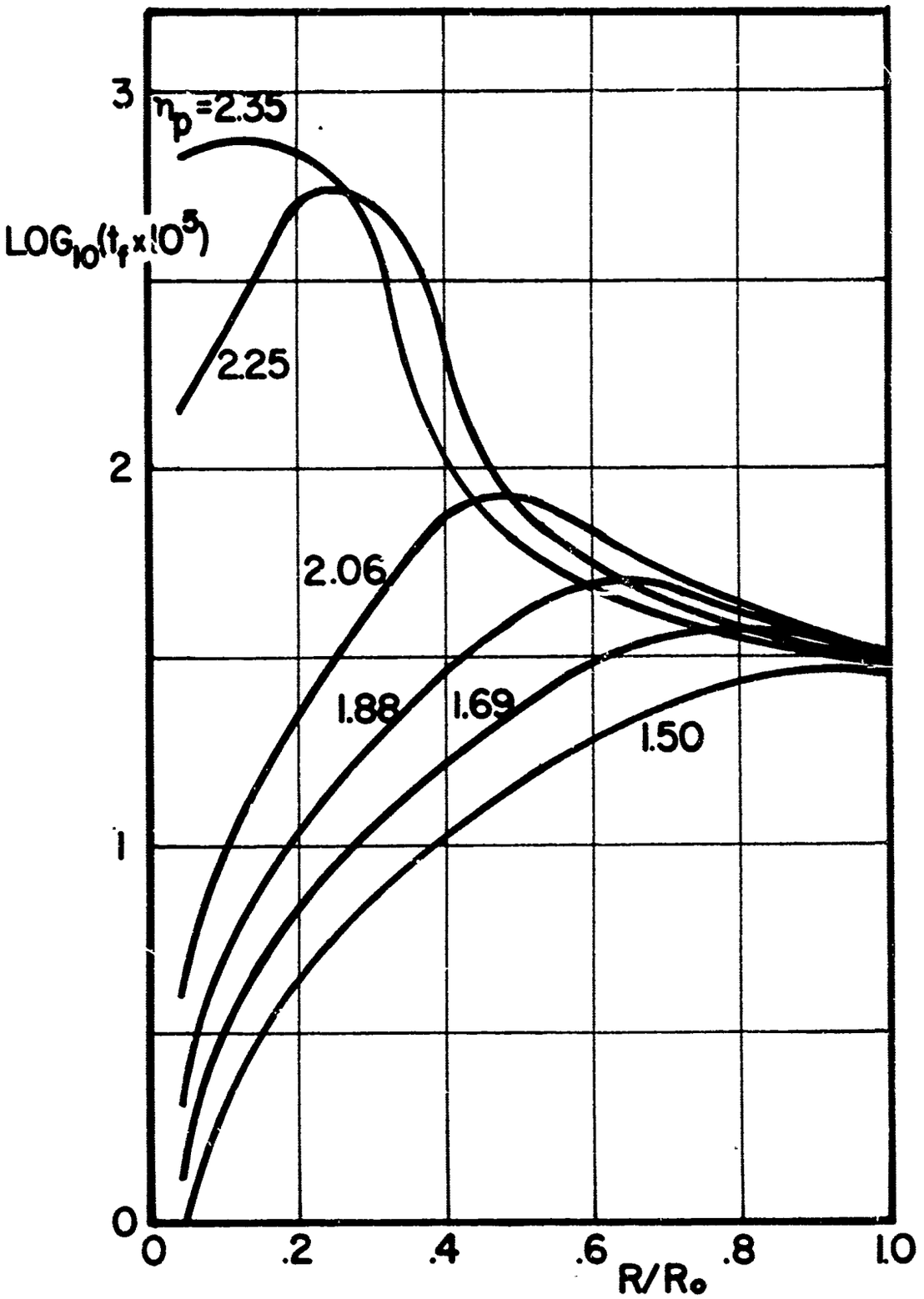

Figure 9. Effect of Center-line Length on the Distribution of Circumferential Fabric Stress.

6. DISCUSSION

In this Section we shall first outline the main conclusions drawn from this work, then discuss questions of accuracy and finally sketch explanations for some of the effects of pulling down the vent.

The principal conclusions to which this work has led are these:

(i) The most spectacular effect of pulling down the vent is the extraordinary decrease in maximum fabric stress, which may be reduced to 10% or less of its value for a flat circular canopy.

(ii) A careful choice of center-line length will give a drag about 18% higher than the drag for the corresponding flat circular canopy at the same speed. The (undeformed) center-line length which accomplishes this is very close to the (undeformed) length of the load lines.

(iii) The cord stress is nearly constant when the center-line length is less than about two skirt radii.

The accuracy of the results may be tested either by comparison with alternative theoretical ways of calculation or by comparison with experiments. A theoretical comparison is shown in Figure 10, where the functions $y(\phi)$ as calculated for two η_p-values, first by the computer program (using a ten-point mesh), and second by the formula (51) are compared. In using (51) the value of t_s was taken from the computer program. The two results are seen to be in excellent agreement and give some confidence in the accuracy of the two procedures for these cases. However, this test is not a severe one.

The more telling comparison is that between theory and experiment. Here the picture is beclouded by the variability of experimental results on

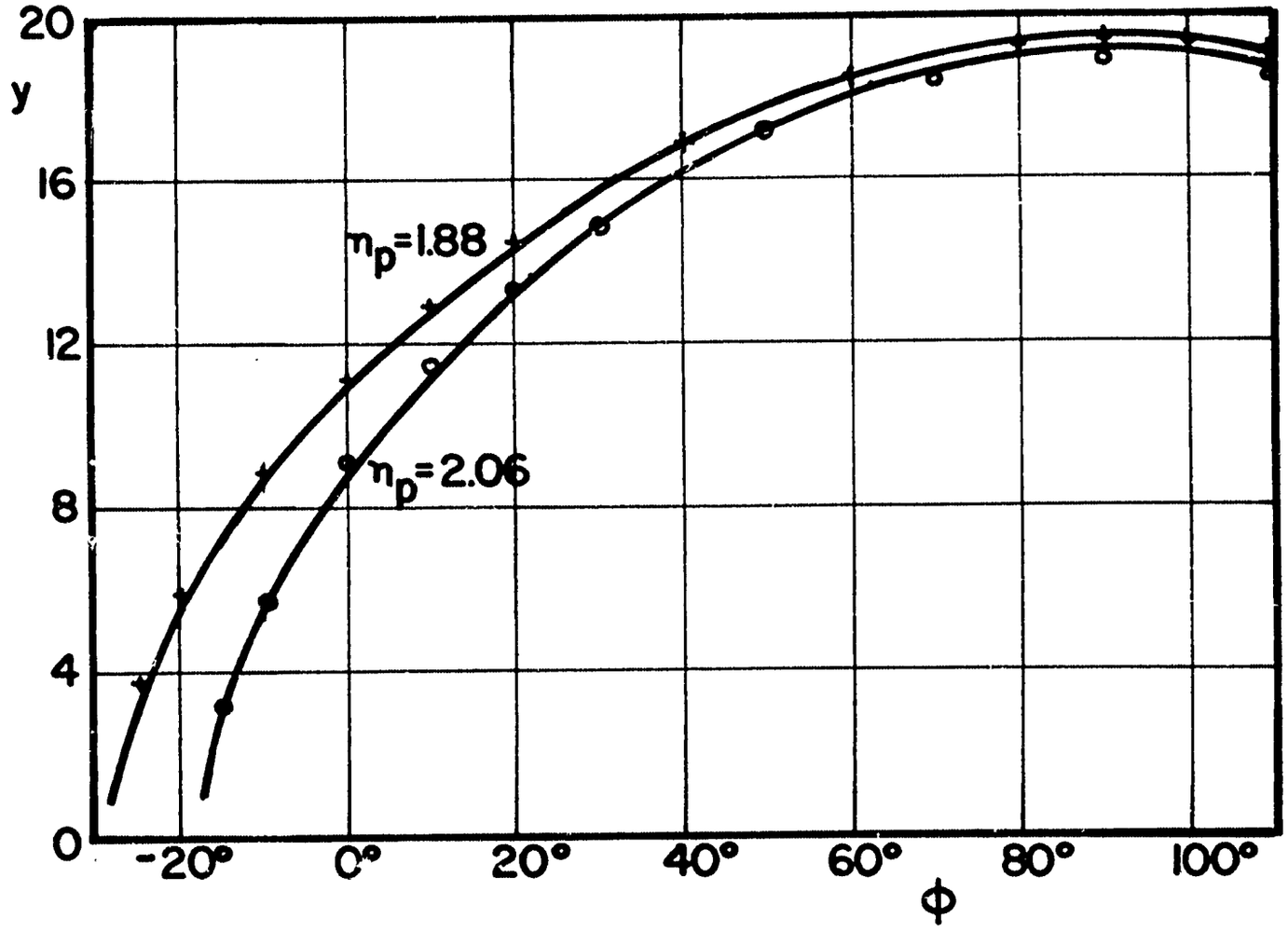

Figure 10. Comparison between the Approximate Solution of Equation (51) and the Computed Values of $y(\phi)$.

parachutes. However, several points are clear. First, experiments on the G-11-A canopy led to the conclusion that the greatest drag was obtained when the center-line length was the same as the load line length (between skirt and load). The theory duplicates this result very closely. Second, the measurement of fabric strain is very difficult, and the author has been unable to find any experimental data dealing with it.

Third, we may present an experiment result [3] and the corresponding theoretical calculation. A flat, circular G-11-A canopy with a load of 5410 lb was found to drop steadily at a speed of 25.5 ft/sec, giving a drag coefficient,

$$C_{D_o} = .883.$$

The same canopy was then modified by installation of a 95-foot centerline and dropped again with the same load. This time, the rate of descent was measured as 24.2 ft/sec, giving

$$C_{D_o} = .980.$$

To duplicate these tests theoretically the program for a flat, circular canopy was first run for a rate of descent, 25.5 ft/sec, and various values of C_p (assumed constant over the canopy) were tried. It was found that

$$C_p \equiv 2.008$$

gave a drag of 5410 lb and a drag coefficient, $C_{D_o} = .883$. The program for the pull-down vent was then run with $C_p \equiv 2.008$, and various velocities were tried, giving the result that the drag (load) was 5410 lb when the rate of descent was 23.7 ft/sec. The corresponding drag coefficient was

$$C_{D_o} = 1.023$$

Hence in this case theory predicted that pulling down the vent would give a 16% increase in C_{D_o}, while the experimental result showed an 11% increase in

C_{D_o}. This agreement is not extremely good, but in view of the uncertainties in measuring rate of descent during full-scale tests, it is not bad.

We conclude that the theory given here is in fairly good agreement with experiment, although we cannot be sure because of the difficulty in obtaining repeatable experimental results. The difference between the drag coefficients of $C_{D_o} = .65$, used for the standard flat circular conditions, and $C_{D_o} = .88$ in the experiments described in this Section is apparently typical of the variability that can occur.

In understanding the mechanics of the pulled-down vent, the main thing we have to explain is the great decrease in maximum fabric stress. We may explain it this way. In the flat, circular canopy the circumferential fabric stress is very high at the vent, and the angle β (the edge angle of the gore) is nearly zero, so that from (9)

$$N_f = E_f \{(r/R) - 1\}.$$

When the vent is pulled down, it is also pulled inward, toward the axis, and (r/R) is reduced, thus reducing N_f near the vent. Thus the high peak of N_f near the vent is knocked down.

We may understand the effect of pull-down on the drag (Figure 5) if we attribute changes in drag to corresponding changes in projected area or maximum radius. For we may integrate (1) to obtain

$$r_{max} = r_i + \int_{R_i}^{R_{max}} f(R') \cos\phi(R') dR',$$

where R_{max} is the R at which r_{max} occurs. Pulling down the vent has two opposite effects on this formula. First, it reduces r_i, and second, it increases

the integral because more of the peak in the cosine function near $\phi = 0$ is included in the integral. For moderate amounts of pull-down the second effect dominates, and r_{max} increases. However, if the vent is pulled down far enough, the first effect takes charge, and r_{max} decreases. This accounts for the general shape of the drag curve in Figure 5.

The author is grateful to E. J. Giebutowski, S. J. Shute, and E. L. Haak of the Airdrop Engineering Laboratory at U. S. Army Natick Laboratories for helpful discussion and suggestions in this work.

REFERENCES

1. Ross, E. W., Jr. "Approximate Analysis of a Flat, Circular Parachute in Steady Descent", U. S. Army Natick Laboratories Report No. 69-51-OSD, December 1968.
2. Hoerner, S. F., "Fluid Dynamic Drag", published by the author, Midland Park, New Jersey, 1958.
3. S. J. Shute, Jr., Private Communication, January 1969.

APPENDIX: NOMENCLATURE

A	Function used in determination of N_c
C_o, C_1, C_2, C_3	Constants in the pressure distribution
C_{D_o}, C_{D_p}	Coefficients of drag, based on flat, circular and projected areas, respectively
C_p	Coefficient of pressure
E_f, E_c	Elastic moduli of fabric and cords
E_p, E_i, E_o	Elastic moduli of center line, vent lines and load lines
f	Extension of cords = $1 + t_s$
G	Number of Gores
H	Function of pressure used in approximate solution
L_i, L_i'	Deformed and undeformed lengths of vent lines
L_o, L_o'	Deformed and undeformed lengths of load lines
L_p, L_p'	Deformed and undeformed lengths of center line
N_f, N_s	Tension forces in fabric and cords
N_c	Equivalent circumferential tension force
N_p	Tension force in control line
p	Net (outward) pressure
q	Dimensionless outward pressure
r, R	Cord radius in deformed and undeformed shapes
R_i, R_o	Vent and skirt radii of undeformed shape
t_f, t_s	Dimensionless fabric and cord stresses (or strains)
t_c	Dimensionless circumferential stress
t_p	Dimensionless stress (or strain) in center line

U	Velocity of steady drop
u_f, u_p, u_o	Dimensionless ratios of elastic moduli
W_L	Weight of the load
w	Dimensionless weight of the load
x	Dimensionless undeformed radius
x_o	Dimensionless skirt radius in undeformed shape
y	Dimensionless deformed radius of cords
Z	Axial distance from vent of points on the cords
z	Dimensionless axial distance of cords from vent

α	Central angle of gores
β	Slope angle of gore where it intersects cords
δ	Depth of gore bulge
η_p	Ratio of center line length to undeformed skirt radius
θ	Angle betweer load lines and canopy axis
λ_i, λ_i'	Dimensionless deformed and undeformed length of vent lines
λ_o, λ_o'	Dimensionless deformed and undeformed lengths of load lines
λ_p, λ_p'	Dimensionless deformed and undeformed lengths of center lines
ρ	Mass density of air
σ'	Contact length between adjacent gores when A > 0
σ	Dimensionless contact length between adjacent gores
ϕ	Angle between cords and horizontal
ϕ_o	Angle between cords and horizontal at skirt

TECHNICAL REPORT DISTRIBUTION

Copies	To
1	Office of the Director, Defense Research and Engineering, The Pentagon, Washington, D. C. 20301
20	Commander, Defense Documentation Center, Cameron Station, Building 5, 5010 Duke Street, Alexandria, Virginia 22314
1	Defense Metals Information Center, Battelle Memorial Institute, Columbus, Ohio 43201
	Chief of Research and Development, Department of the Army, Washington, D. C. 20310
2	ATTN: Physical and Engineering Sciences Division
	Commanding Officer, Army Research Office (Durham), Box CM, Duke Station, Durham, North Carolina 27706
1	ATTN: Information Processing Office
	Commanding General, U. S. Army Materiel Command, Washington, D. C. 20315
1	ATTN: AMCRD-RC-M
	Commanding General, U. S. Army Electronics Command, Fort Monmouth, New Jersey 07703
2	ATTN: AMSEL-RD-MAT
	Commanding General, U. S. Army Missile Command, Redstone Arsenal, Alabama 35809
1	ATTN: Technical Library
	Commanding General, U. S. Army Munitions Command, Dover, New Jersey 07801
1	ATTN: Technical Library
1	Technical Library U. S. Army Natick Laboratories Natick, Massachusetts 01760
	Commanding General, U. S. Army Satellite Communications Agency, Fort Monmouth, New Jersey 07703
1	ATTN: Technical Document Center
	Commanding General, U. S. Army Weapons Command. Research and Development Directorate, Rock Island, Illinois 61201
1	ATTN: AMSWE-RDR
	Commanding General, White Sands Missile Range, New Mexico 88002
1	ATTN: STEWS-WS-VT

Copies	To
	Commanding Officer, Aberdeen Proving Ground, Maryland 21005
1	ATTN: Technical Library, Building 313
	Commanding Officer, Frankford Arsenal, Bridge and Tacony Streets, Philadelphia, Pennsylvania 19137
1	ATTN: Library Branch C 2500
	Commanding Officer, Department of the Army, Ohio River Division Laboratories, Corps of Engineers, 5851 Mariemont Avenue, Cincinnati, Ohio 45227
1	ATTN: ORDLB-TR
	Commanding Officer, Picatinny Arsenal, Dover, New Jersey 07801
1	ATTN: SMUPA-VA6
	Commanding Officer, Redstone Scientific Information Center, U. S. Army Missile Command, Redstone Arsenal, Alabama 35809
4	ATTN: AMSMI-RBLD, Document Section
	Commanding Officer, Watervliet Arsenal, Watervliet, New York 12189
1	ATTN: SWEWV-RDT, Technical Information Services Office
	Commanding Officer, U. S. Army Aeromedical Research Unit, P O. Box 577, Fort Rucker, Alabama 36460
1	ATTN: Technical Library
1	Commanding Officer, U. S. Army Aviation Materiel Laboratories, Fort Eustis, Virginia 23604
	Director, Naval Research Laboratory, Anacostia Station, Washington, D. C. 20390
1	ATTN: Technical Information Officer
	Chief, Office of Naval Research, Department of the Navy, Washington, D. C. 20315
1	ATTN; Code 423
	Headquarters, Aeronautical Systems Division, Wright-Patterson Air Force Base, Ohio 45433
5	ATTN: ASRCEB
1	U. S. Atomic Energy Commission, Office of Technical Information Extension, P.O. Box 62, Oak Ridge, Tennessee
	National Aeronautics and Space Administration, Washington, D. C. 20546
1	ATTN: Mr. B. G. Achhammer
1	Mr. G. C. Deutsch
1	Mr. R. V. Rhode

Copies To

National Aeronautics & Space Administration, Marshall Space Flight Center, Huntsville, Alabama 35812
1 ATTN: R-P&VE-M, Dr. W. R. Lucas
1 M-F&AE-M, Mr. W. A. Wilson, Building 4720

Commanding Officer, U.S. Army Materials & Mechanics Research Center, Watertown, Massachusetts 02172
1 ATTN: Mr. J. F. Mescall
1 Mr. J. I. Bluhm
1 Mr. O. L. Bowie
1 Mr. R. B. Beeuwkes

National Aeronautics & Space Administration, Langley Research Center, Hampton, Virginia 23365
1 ATTN: Dr. R. W. Leonard

1 President
US Army Airborne Electronics & Special Warfare Board
Fort Bragg, North Carolina 28307

Commanding General
U.S. Army Materiel Command, Washington, DC 20315
1 ATTN: AMCRD-F

1 Commanding Officer, 6511th Test Group (Parachute), Naval Air Facility, El Centro, California 92243

Commander, Wright Patterson Air Force Base, Dayton, Ohio 45433
1 ATTN: FDFR

University of Minnesota, Department of Aeronautics & Engineering Mechanics, Minneapolis, Minnesota 55414
1 ATTN: Dr. H. G. Heinrich

Unclassified
Security Classification

DOCUMENT CONTROL DATA - R & D

(Security classification of title, body of abstract and indexing annotation must be entered when the overall report is classified)

1. ORIGINATING ACTIVITY (Corporate author)	2a. REPORT SECURITY CLASSIFICATION
US Army Natick Laboratories Natick, Massachusetts 01760	Unclassified
	2b. GROUP

3. REPORT TITLE

ANALYSIS OF A PARACHUTE WITH A PULLED-DOWN VENT

4. DESCRIPTIVE NOTES (Type of report and inclusive dates)

5. AUTHOR(S) (First name, middle initial, last name)

Edward W. Ross, Jr.

6. REPORT DATE	7a. TOTAL NO. OF PAGES	7b. NO. OF REFS
February 1969	34	3

8a. CONTRACT OR GRANT NO.	9a. ORIGINATOR'S REPORT NUMBER(S)
b. PROJECT NO. 1F162203D195	69-71-OSD
c.	9b. OTHER REPORT NO(S) (Any other numbers that may be assigned this report)
d.	

10. DISTRIBUTION STATEMENT

This document has been approved for public release and sale; its distribution is unlimited.

11. SUPPLEMENTARY NOTES	12. SPONSORING MILITARY ACTIVITY
	US Army Natick Laboratories Natick, Massachusetts 01760

13. ABSTRACT

The previous analysis of the author for flat circular canopies in steady descent is here extended to deal with canopies having a pulled-down vent. A general theory is developed, and a partial, approximate solution is found in closed form for certain conditions. The general theory is taken as the basis of a computer program. An example is worked out to demonstrate the use of the program in determining the optimum length of center line. The results are compared with tests and fairly good agreement is obtained. The most interesting outcome is the prediction that the maximum fabric stress is greatly reduced by pulling the vent down.

DD FORM 1 NOV 65 1473 REPLACES DD FORM 1473, 1 JAN 64, WHICH IS OBSOLETE FOR ARMY USE.

Unclassified
Security Classification

14. KEY WORDS	LINK A		LINK B		LINK C	
	ROLE	WT	ROLE	WT	ROLE	WT
Stress analysis	8					
Length	6					
Parachute lines	6					
Center	0					
Vents	6					
Fabrics	7					
Stresses	7					
Shape	7					
Parachutes	9					
Computer programs	10					